Tellus (2001), 53A, 380–402
Printed in UK. 


TELLUS
ISSN 0280–6495

# Infrared atmospheric sounding interferometer data information content; instrument characterization and the impact of a priori information

By P. PRUNET[1]*, V. CASSÉ[2] and J.-N. THÉPAUT[2], [1]*NOVELTIS, Parc Technologique du Canal, 31520 Ramonville Saint-Agne, France;* [2]*Centre National de Recherches Météorologiques, Météo-France, 31057 Toulouse Cedex, France*

(Manuscript received 21 April 1998; in final form 23 November 2000)

ABSTRACT

The use of linear estimation for the study of the information content of a given satellite radiance data set for temperature and humidity profile retrievals is first reviewed. A particular formulation of the retrieval approach is then used to obtain an intrinsic characterisation of the Infrared Atmospheric Sounding Interferometer (IASI) data set, in terms of accuracy versus vertical resolution of retrieved profiles. The performance of the IASI instrument alone is analysed and compared to that of the currently-used HIRS-TOVS. The problem is then regularized by addition of a priori independent information to the initial data set. The potential use of IASI data for some particular choices of the a priori information associated with practical problems such as profile inversion or data assimilation for weather forecasting is analysed. The approach is finally used to derive an "empirical" objective framework to define the vertical discretization adapted to these problems.

## 1. Introduction

For more than two decades, radiance measurements by satellite-borne multispectral infrared radiometers have been used to remotely sense atmospheric temperature and moisture profiles (Kaplan, 1959; Smith and Wolf, 1976). Because the radiances arise from thick layers of the atmosphere, the poor vertical resolution and associated accuracy of the derived profiles limit their use in numerical weather prediction (Thépaut and Moll, 1990; Prunet et al., 1998). The poor vertical resolution of current operational satellite sounding instruments is attributable, in part, to a low spectral resolution. Due to this coarse spectral resolution, the radiometer does not separately sense radiation between absorption lines (Kaplan et al., 1977). To approach the ultimate vertical sounding resolution and accuracy achievable with passive instruments, a new generation of high-spectral-resolution observing systems are proposed, based on large-detector-array grating spectrometer like the Advanced Infrared Sounder (AIRS; Chahine, 1991), or on Michelson interferometers like the IASI instrument (Diebel et al., 1996). Such developments will have a significant impact on future remote sensing science missions and on the improvements of atmospheric process understanding and prediction. To quantify the potential of these new observing systems, one needs developments of tools and schemes to quantitatively analyse their performances in a scientifically consistent and objective manner.

Modern techniques for objective analysis of satellite observations that account realistically for

* Corresponding author.
e-mail: pascal.prunet@noveltis.fr

the measurements share a common Bayesian statistical framework with techniques for retrieving atmospheric profile information from radiance data (Lorenc, 1986), in the way that they deduce the "best" estimate of the state of the atmosphere, given a set of measurements together with any appropriate prior informations that may be available about the system. There are two distinct aspects to this question, which may be described as the "inverse" problem and the "estimation" problem (Rodgers, 1976b). The former is the problem of inverting a known functional relationship between the radiance data and the atmospheric state so as to express that state in terms of the data. The latter concerns the treatment of errors, ill-conditioning and underconstraint that arise in dealing with most of the radiance data inversion problems. This treatment consists in modifying the initial inverse problem by adding some independent information in order to obtain a physically plausible solution, and is known as the regularization of the inverse problem (Hansen, 1998, and references therein).

This paper will use a linearized version of the radiative transfer equation so that the inverse problem is straightforward, and focuses on the questions associated with the estimation problem: understanding and describing the information content of the radiance measurements. The term "information content" is not used here strictly in the sense of information theory (Shannon, 1949), but as some estimation of the quality, in terms of precision and accuracy, of the atmospheric state retrieved from the data, by the analysis of the relationships between the true atmospheric state and the one retrieved using inverse methods, and the error analysis of the retrieved state. The techniques of linear optimal estimation and the general methods of regularization developed by Tikhonov (1963) and Twomey (1963), along with the theoretical vertical resolution analysis (Backus and Gilbert, 1970; Conrath, 1972; Purser and Huang, 1993) and error analysis (Rodgers, 1990) are used in a common framework to quantify and compare, in a case study, the information content of data from two different sounding instruments: the future high-spectral-resolution IASI instrument proposed in the context of the METOP program on the forthcoming European polar platform (EPS); and the currently operational HIRS-TOVS radiometer aboard the NOAA satellites.

The linear inverse problem, the methodology and some well-known techniques of regularization of the retrieved solution are first described and included in a common formalism, in an approach to the information content study of satellite data which allows a controlled compromise between accuracy and vertical resolution of the atmospheric state reconstructed from these data, and inclusion of independent informations on the atmospheric state (Section 2). This methodology is then first applied to quantify the vertical resolution and accuracy provided by the IASI sounding instrument, and to compare it with that of the HIRS-TOVS radiometer (Section 3.1). Inclusion of independent information is then examined, and the potential performance of the IASI data utilization in particular applications such as temperature and humidity profile inversions or data assimilation for numerical weather prediction are studied (Section 3.2). Finally concluding remarks are given in Section 4.

## 2. Methodology

When it is possible, the unified notation proposed by Ide et al. (1997) for data assimilation is respected in this section. Deducing atmospheric information from radiance data requires the inversion of the radiative transfer equation (RTE) (Rodgers, 1976a; Rochard, 1979). For the purpose of discussing information content, the non-linearity of the RTE is not a major issue. We focus on the linearized discrete radiative transfer equation, where the measurement vector $\boldsymbol{y}$ is related to the vector $\boldsymbol{x}$ representing the atmospheric state such that:

$$\boldsymbol{y} - \boldsymbol{y}^0 = \boldsymbol{H}(\boldsymbol{x} - \boldsymbol{x}^{\circ}) + \varepsilon \Leftrightarrow \boldsymbol{d} = \boldsymbol{H}\boldsymbol{f} + \varepsilon, \tag{1}$$

where $\boldsymbol{y}^0$ and $\boldsymbol{x}^0$ define some arbitrary linearization point. $\boldsymbol{H}$ is the linearised radiative transfer operator, i.e., the $m \times n$ matrix of the so-called weighting functions, and $\varepsilon$ is the data noise vector: eq. (1) is the matrix formulation which approximate the Fredholm linear integral equation of the first kind. $\boldsymbol{d}, \boldsymbol{y}, \boldsymbol{y}^0$ and $\varepsilon$ are $m$-vectors defined on $\Re^m$, hereafter named the data space, and $\boldsymbol{f}$, $\boldsymbol{x}$ and $\boldsymbol{x}^0$ are $n$-vectors defined on $\Re^n$, hereafter named the parameter space. The data noise $\varepsilon$ is supposed to be unbiased and with known covariance matrix $\boldsymbol{R}$. One attempts to find a solution to eq. (1) by linear inversion. The principle of any linear inversion method is to obtain an estimate $\hat{f}$ of $f$ as a linear combination of the measurements $d$:

$$\hat{f} = = Kd,$$

where matrix $K$ can be viewed as a general linear inverse of $H$. By taking account of (1)

$$\hat{f} = Gf + K\varepsilon, \qquad G = KH. \tag{3}$$

One attempts to construct $K$ such that $\hat{f}$ is a physically plausible solution as close as possible to $f$ (that is, $G$ approaches the $n \times n$ identity matrix $I_n$), in such a manner that it prevents noise from contaminating the parameter estimates (i.e., $K$ approaches the null matrix $\mathbf{0}_{nm}$). There is consequently a trade-off relationship between the sharpness of the solution and its accuracy. Eq. (3) characterizes how $f$ (the departure of the true profile from the linearization point) is smoothed by the retrieval process, and the matrix $G$ indicates the form of filtering which has been performed. This matrix is named the model resolution matrix (Menke, 1984; Ory and Pratt, 1994). The retrieval at any level j is an average of the whole true profile weighted by the $j$th row of $G$, and the rows of $G$ are named the averaging kernels. From (3), the quality of the solution estimate $f$ can be characterized by two main indicators: the noise of the solution, which depends on the general inverse $K$ and on the data noise ε, and the smoothing properties of the model resolution matrix $G$. The measure of this smoothing is associated with the concept of resolution, which may have many possible definitions (Backus and Gilbert, 1968; Thompson, 1982; Purser and Huang, 1993). Since the model resolution matrix would be ideally equal to $I_n$, the resolution associated with the retrieval problem is generally characterized by some measure of the distance between $G$ and $I_n$.

### 2.1. Solution of the linear problem

One has to define some metrics on the data and parameter spaces. We define scalar products and norms by using the symmetric, positive definite, matrices $M$ ($m \times m$) *and* $N$ ($n \times n$) on $\Re^m$ and $\Re^n$, respectively, such as

$$\begin{aligned} \|g\|^2_{\mathrm{M}} &= [d, Md] = d^{\mathrm{T}}Md, \\ \|f\|^2_{\mathrm{N}} &= [f, Nf] = f^{\mathrm{T}}Nf, \end{aligned} \tag{4}$$

where T stands for the transpose. In the case of the study of the radiative transfer problem, it is convenient to use the data error covariance matrix $R$ for the definition of the data space metric. Then one defines $M^{-1} = R$.

The rank $k$ of the system is lower than the minimum of $m$ and $n$. In order to solve the over-determination of (1), one minimizes the following objective function:

$$\Omega(f) = \|Hf - d\|^2_{\mathbf{R}^{-1}}. \tag{5}$$

The minimum is obtained for a solution $\hat{f}$ such that

$$H^{\mathrm{T}}R^{-1}d = H^{\mathrm{T}}R^{-1}H\hat{f}. \tag{6}$$

Due to the under-determination of (1), the matrix $H^{\mathrm{T}}R^{-1}H$ is often singular and non-invertible. Then the generalised solution (6) has to be regularized. It exists various regularization techniques (for a thorough description of these methods, see for example Rodgers, 1976a; Rochard, 1979; Hansen, 1998). We describe below two forms of regularization. In this two cases, the regularization is driven by the parameter space metric $N$.

### 2.2. Tikhonov regularization

The so-called Tikhonov regularization methods consist in adding to the data some independent a priori information, in order to reconstruct the complete solution (i.e., to estimate each component of the vector $f$). In the general form, the Tikhonov regularization (TR) consists in minimizing the objective function

$$\Omega_{\mathrm{TR}}(f) = \|Hf - d\|^2_{\mathbf{R}^{-1}} + \gamma\|f\|^2_{\mathrm{N}}, \tag{7}$$

which finds a compromise between the misfit between the solution and the data on one hand, and the norm of the solution on the other hand, controlled by the regularization parameter $\gamma$. The constraint on the solution norm represents the a priori information introduced in the system. The form of this prior information is fixed by $N$ and $x^0$, while $\gamma$ control the importance of prior information in the retrieval process. The joint constrained minima of misfit and solution norm bear an inverse, or trade-off, relationship, as a function of $\gamma$, which is also called a trade-off parameter. Minimizing (7) gives the solution

$$\hat{f}_{\mathrm{TR}} = (H^{\mathrm{T}}R^{-1}H + \gamma N)^{-1}H^{\mathrm{T}}R^{-1}d. \tag{8}$$

At the limit $\gamma = 0$, there is no regularization and one obtains the solution (6) which gives the minimum possible misfit. Increasing $\gamma$ leads to an increase in this misfit while decreasing the noise on the solution.

One can associate with the general TR solution an estimate of the error on this solution, under the form of an "analysis" error covariance matrix $\boldsymbol{A}$ (Tarantola and Valette, 1982; Lorenc, 1986):

$$\boldsymbol{A} = (\boldsymbol{H}^{\mathrm{T}}\boldsymbol{R}^{-1}\boldsymbol{H} + \gamma\boldsymbol{N})^{-1} \tag{9}$$

and the generalized inverse within the TR formalism is given by:

$$\boldsymbol{K}_{\mathrm{TR}} = (\boldsymbol{H}^{\mathrm{T}}\boldsymbol{R}^{-1}\boldsymbol{H} + \gamma\boldsymbol{N})^{-1}\boldsymbol{H}^{\mathrm{T}}\boldsymbol{R}^{-1}. \tag{10}$$

### 2.3. *Mollifier regularization*

Mollifier regularization is the general formalism from which the Backus Gilbert approach (Backus and Gilbert, 1970) can be seen as a particular variant (Hansen, 1998). Considering each averaging kernel $\boldsymbol{g}^j$ of the system (each row of $\boldsymbol{G}$) given by

$$\boldsymbol{g}^{j\mathrm{T}} = \boldsymbol{e}^{j\mathrm{T}}\boldsymbol{G} = \boldsymbol{e}^{j\mathrm{T}}\boldsymbol{K}\boldsymbol{H} = \boldsymbol{k}^{j\mathrm{T}}\boldsymbol{H}, \tag{11}$$

with

$$\boldsymbol{k}^{j\mathrm{T}} = \boldsymbol{e}^{j\mathrm{T}}\boldsymbol{K}, \tag{12}$$

where $\boldsymbol{e}^j$ is the unitary vector pointing at level $j$, mollifier methods consist in solving the local problem of finding an estimate of the atmospheric state at level $j$

$$\hat{\boldsymbol{f}}^j = \boldsymbol{e}^{j\mathrm{T}}\boldsymbol{K}\boldsymbol{H}\boldsymbol{f} + \boldsymbol{e}^{j\mathrm{T}}\boldsymbol{K}\varepsilon = \boldsymbol{g}^{j\mathrm{T}}\boldsymbol{f} + \boldsymbol{k}^{j\mathrm{T}}\varepsilon, \tag{13}$$

such that the averaging kernel $\boldsymbol{g}^j$, which acts as a "smoother" weighting vector of the true atmospheric state, is as close as possible to a fixed "ideal" weighting vector $\boldsymbol{p}^j$. We consider here only cases where the ideal form $\boldsymbol{p}^j$ of $\boldsymbol{g}^j$ is $\boldsymbol{e}^j$, the unitary vector pointing at level $j$ (that is, finding $\boldsymbol{G}$ as close as possible to $\boldsymbol{I}_n$). Mollifier methods are then essentially regularization methods in which the ideal form of $\boldsymbol{g}^j$ is specified, from which the $\boldsymbol{k}^j$ is computed. These methods are different from the Tikhonov regularization in that they examine what can be said about the solution given only the observations. Thus, by their intrinsic smoothing of the solution through the weighting vector $\boldsymbol{g}^j$, they basically consist in decreasing the dimension of the solution $n$ to the rank of the problem $k$. The mollifier regularization (MR) consists in minimizing the objective function

$$\Omega_{\mathrm{MR}}(\boldsymbol{k}^j) = \|\boldsymbol{H}^{\mathrm{T}}\boldsymbol{k}^j - \boldsymbol{e}^j\|^2_{\mathbf{N}^{-1}} + \gamma\|\boldsymbol{k}^j\|^2_{\mathbf{R}} \quad \text{at each level } j, \tag{14}$$

which finds a compromise between the misfit of the averaging kernels $\boldsymbol{G}$ to the $n \times n$ identity matrix and the norm of $\boldsymbol{k}^j$, controlled by the trade-off parameter $\gamma$. Note that the regularization term can be rewritten as

$$\|\boldsymbol{k}^j\|^2_{\mathbf{R}} = \boldsymbol{e}^{j\mathrm{T}}\boldsymbol{K}\boldsymbol{R}\boldsymbol{K}^{\mathrm{T}}\boldsymbol{e}^j \tag{15}$$

and as such, it is the noise on the solution at the level $j$. On the other hand, the misfit between $\boldsymbol{G}$ and $\boldsymbol{I}_n$ is a measure of the smoothing properties of $\boldsymbol{G}$, in the sense of the $\boldsymbol{N}^{-1}$-norm measure. The MR problem realises a compromise between smoothing of the solution and noise on this solution. One can plot the smoothing versus noise as a function of $\gamma$, and obtain a trade-off curve which is a powerful analysis tool (Backus and Gilbert, 1970; Conrath, 1972; Rodgers, 1976a, 1976b). The minimization of (14) leads to the solution:

$$\boldsymbol{k}^{j\mathrm{T}}_{\mathrm{MR}} = \boldsymbol{e}^{j\mathrm{T}}\boldsymbol{N}^{-1}\boldsymbol{H}^{\mathrm{T}}(\boldsymbol{H}\boldsymbol{N}^{-1}\boldsymbol{H}^{\mathrm{T}} + \gamma\boldsymbol{R})^{-1}, \tag{16}$$

$$\hat{\boldsymbol{f}}^j_{\mathrm{MR}} = \boldsymbol{k}^{j\mathrm{T}}_{\mathrm{MR}}\boldsymbol{d}. \tag{17}$$

Then the TR (7) and MR (14) formulations with the same metric $\boldsymbol{N}$ and the same choice for the value of the trade-off parameter $\gamma$, give the same answer, i.e.,

$$\boldsymbol{k}^{j\mathrm{T}}_{\mathrm{MR}} = \boldsymbol{e}^{j\mathrm{T}}\boldsymbol{K}_{\mathrm{TR}}, \qquad \hat{\boldsymbol{f}}^j_{\mathrm{MR}} = \boldsymbol{e}^{j\mathrm{T}}\hat{\boldsymbol{f}}_{\mathrm{TR}}, \tag{18}$$

which was already shown in a more general formalism (Yanovskaya and Ditmar, 1990; Rodi, 1991). At the limit $\gamma = 0$ for the MR formulation, there is no regularization, and one obtains the solution (6).

There is a conceptual difference between Tikhonov and mollifier approaches. TR provides an estimate of the whole profile (i.e., an estimate of each component of the $n$-vector $\boldsymbol{f}$, given the parameter space discretization defined a priori) by adding a priori information and minimizes the associated noise estimate (which is the combination of noises coming from data and a priori informations). MR provides an estimate of a smoothed profile, given only the data, by computing the weakest possible smoothing (in the sense of a given measure of this smoothing), while the associated noise comes only from the data. This two conceptual approaches of the regularization allow us to introduce two physically significant ways for the consistant regularization of our inversion problem.

### 2.4. *Instrument characterization: controlling the vertical resolution of the retrieval*

The vertical resolution associated with the retrieval is defined as a measure of the smoothing properties of $\boldsymbol{G}$. Starting with the molifier formalism, the resolution is directly defined from the choice of the metric $\boldsymbol{N}$. Above results for TR or MR formulations are also valid when $\|\cdot\|_{\mathbf{N}^{-1}}$ is a semi-norm, i.e., when $\boldsymbol{N}^{-1}$ is positive but not definite (Ory and Pratt, 1994; Hansen, 1998; Rodi, 1991). Such semi-norms, as well as their counterparts in the TR formalism, measure geometrical properties of the averaging kernels or of the profiles. This geometrical measure does not allow to work with a multi-profile atmospheric state vector $\boldsymbol{x}$ dealing with different units. MR or TR approaches used with such metrics will thus be applied separately on each profile part of the state vector $\boldsymbol{x}$ (temperature profile alone and humidity profile alone, for example) to investigate the information content of radiance data. Useful definitions of the resolution, based on the measurement of the spread of the averaging kernels, were introduced as semi-norms in the MR formulation (Backus and Gilbert, 1968, 1970; Johnson and Gilbert, 1972; Rodi, 1991). Johnson and Gilbert (1972) proposed the following definition for the spread of the averaging kernel at level $j$:

$$s_{\mathrm{h}}^{j} = 12 \sum_{k=1}^{n} \left[ \sum_{l=k}^{n} g^{jl} - U(z^{j} - z^{k}) \right]^{2}, \tag{19}$$

where $g^{jl}$ is the $l$th element of the averaging kernel vector, and where $U$ is the Heaviside function. The Johnson–Gilbert measure shares the essential properties of the original Backus–Gilbert spread, i.e., when $\boldsymbol{g}^{j}$ is of Gaussian, Lorentzian, box, or triangular form, $s_{\mathrm{h}}^{j}$ gives the full width at half maximum of the averaging kernel at level $j$. If the Johnson–Gilbert spread is substituted into the constrained minimization problem (14) (i.e., replacing the first right-hand term in (14) by $s_{\mathrm{h}}^{j}$), one defines a family of solutions as a function of level $j$ and trade-off parameter $\gamma$. As shown by Rodi (1991) for the continuous problem, this regularization problem is equivalent (in the sense of the formulation (18)) to the Tikhonov regularization, where the semi-norm $\boldsymbol{N}$ is the discrete approximation of the first vertical derivative operator (Rodi, 1991; Press et al., 1992, §18.5 for a description of $\boldsymbol{N}$ in this case).

The concept of vertical resolution is thus associated with the smoothing properties of the retrieval method, and is defined here by the measurement of the spread of the averaging kernels. The notion of resolution is linked to the associated noise on the solution: degradation of the resolution (the smoothing of the retrieval by the increase of the spread at each atmospheric level in the MR formalism , and equivalently by the increase of prior information in the TR formalism) is associated with the decrease of noise on the retrieved profile.

### 2.5. *Optimal atmospheric profile retrieval: adding statistical prior information*

The TR formalism may be used for the addition of independent information available for the atmosphere to the data. Prior statistics for the behavior of the atmosphere are always available, with more or less accuracy depending on the context of the problem. For temperature and humidity profile estimates, prior information may be obtained, for example, from a climatological database covering a large range of typical temperature and humidity profiles over the whole atmosphere. Statistics computed from such a database will give our "minimum" knowledge of atmospheric behavior. In the context of profile inversion from radiance measurements, air mass selection from this database will give improved statistics. In the context of using radiance data for assimilation in a weather forecasting system, statistics provided by the numerical model will be available. An estimation of the information content of a given data set which takes into account such statistical prior information is then of obvious practical interest.

If these prior statistics are used as regularization constraints, the problem becomes well-posed, and a solution is usually possible without further constraint. The TR formulation allows one to introduce such statistical prior knowledge as a constraint on the solution, by replacing the norm $\boldsymbol{N}$ in the TR formulation with the inverse of the error covariance matrix characterizing the a priori statistics, and by taking $\gamma$ equal to 1. One obtains in this case, the best linear unbiased estimate (BLUE), which minimizes the trace of the analysis error covariance matrix $\boldsymbol{A}$, given a set of data $\boldsymbol{y}$ with error covariance matrix $\boldsymbol{R}$ and a reference atmospheric state $\boldsymbol{x}^{\mathrm{b}}$ known with an error covariance matrix $\boldsymbol{B}$ (and the associated reference point $\boldsymbol{y}^{\mathrm{b}}$ in the data space). If the probability density functions (p.d.f.) associated with the data and the reference atmospheric state are Gaussian, the BLUE has also a Gaussian p.d.f. and its covariance matrix is given by (9) with $\gamma=1$ and $\boldsymbol{N}=\boldsymbol{B}^{-1}$. Rodgers (1990) provides a useful formulation of this retrieval error. He shows that $\boldsymbol{A}$ can be written as the sum of two terms:

$$\boldsymbol{A}=\boldsymbol{A}_{\mathrm{b}}+\boldsymbol{A}_{m}=(\boldsymbol{I}-\boldsymbol{K}_{\mathrm{TR}}\boldsymbol{H})\boldsymbol{B}(\boldsymbol{I}-\boldsymbol{K}_{\mathrm{TR}}\boldsymbol{H})^{\mathrm{T}} + \boldsymbol{K}_{\mathrm{TR}}\boldsymbol{R}\boldsymbol{K}_{\mathrm{TR}}^{\mathrm{T}}, \quad (20)$$

where $\boldsymbol{K}_{\mathrm{TR}}$ is obtained from (10) with $\gamma\boldsymbol{N}=\boldsymbol{B}^{-1}$. The $\boldsymbol{A}_{\mathrm{b}}$ term can be defined as the smoothing error, and the $(\boldsymbol{I}-\boldsymbol{K}_{\mathrm{TR}}\boldsymbol{H})$ operator defines the part of the parameter space for which no information is available from the measurements, and for which the error is the a priori error. The $\boldsymbol{A}_m$ term is the measurement noise component error. The BLUE is given by the TR solution (8) with $\boldsymbol{d}=\boldsymbol{y}-\boldsymbol{y}^{\mathrm{b}}$ and $\boldsymbol{f}=\boldsymbol{x}-\boldsymbol{x}^{\mathrm{b}}$. In this case the regularization is fixed by the a priori information on the reference state $\gamma\boldsymbol{N}=\boldsymbol{B}^{-1}$.

The BLUE solution may be equivalently obtained in MR formulation by using the prior statistics as an extra set of measurements at high resolution (Rodgers, 1976b), whose value is equal to the statistical mean of the prior knowledge, and whose error is given by the associated error covariance matrix. Since statistics are given at each discrete level of our problem, the weighting functions we attach to them will be represented by the $\boldsymbol{I}_n$ matrix (saying that we have a prior estimate of each element of the profile). As before, the problem without further constraint becomes well-posed, and the resolution of the MR minimization (14) with $\gamma=0$ will give the BLUE solution, without any smoothing of the profile, and a noise estimate given by (15).

## 3. Applications to the study of HIRS-TOVS and IASI data information content

In the context of an information content analysis of a given remote sounding instrument (or more generally of any set of data), MR and TR approaches provide a framework for the estimation of the information content of the data only, and of the capabilities of the instrument itself. These methods should also be used to estimate the necessary quality of the a priori information required to obtain a given performance in the analysis of the atmospheric state with the instrument, or for the estimation of the information content of the data used with other information in a particular application. Applications of TR and MR methods are illustrated below in the context of the information content analysis of the high spectral resolution IASI infrared remote sensor sounder for EPS/Metop. The information content of the HIRS-TOVS instrument aboard the NOAA satellites is also examined for comparison with IASI performances, as has been done by Prunet et al. (1998).

The IASI instrument has 8460 channels covering most of the thermal infrared, with an unapodised spectral resolution of 0.25 $\mathrm{cm}^{-1}$ between 645 $\mathrm{cm}^{-1}$ and 2760 $\mathrm{cm}^{-1}$ (Diebel et al., 1996). The HIRS-TOVS has 19 spectral channels (Smith et al., 1979). For the purpose of comparison with IASI, one considers the channels used in the ECMWF operational system, i.e., channels 1–7 covering the 15 μm band, channels 10–12 between 6.7 and 8.3 μm for water vapor sounding, and channels 13–15 in the 4.3 μm band (Smith et al., 1979, for further details on these channels).

For each instrument, the measurement vector $\boldsymbol{y}$ consists of the brightness temperature in each of the corresponding spectral intervals. The state vector $\boldsymbol{x}$ contains surface temperature, and temperature and water vapor specific humidity at each of the 39 vertical levels given in Table 1. For this case study, the atmosphere is assumed to be cloudless, the surface to be black, other atmospheric constituents to be constant, and an arbitrary meteorological situation is considered. The well-studied Floyd case of 10 September 1993, 12 UTC, was chosen (Rabier et al., 1996, for its description), and a particular profile $\boldsymbol{x}^0$ (Prunet et al., 1998) is taken from the ECMWF operational analysis state of this situation and used as the linearization point in our study. To help the discussion of the results presented below, the discretized atmospheric column is separated into four specific regions, according to the structure of the temperature profile. These regions, namely the troposphere, the tropopause, the stratosphere, and upper layers, are defined in Table 1.

Table 1. *Discretized vertical levels on which the atmospheric state is represented, and corresponding vertical regions of the atmosphere*

| Levels | Height (km) | Region | Levels | Height (km) | Region |
|---|---|---|---|---|---|
| 1 | 69.6 | upper | 21 | 14.5 | tropopause |
| 2 | 65.7 | upper | 22 | 13.1 | tropopause |
| 3 | 61.2 | upper | 23 | 11.8 | tropopause |
| 4 | 57.2 | upper | 24 | 11.1 | troposphere |
| 5 | 52.5 | upper | 25 | 10.4 | troposphere |
| 6 | 47.8 | stratosphere | 26 | 9.7 | troposphere |
| 7 | 44.6 | stratosphere | 27 | 9.0 | troposphere |
| 8 | 41.6 | stratosphere | 28 | 8.3 | troposphere |
| 9 | 38.7 | stratosphere | 29 | 7.5 | troposphere |
| 10 | 35.8 | stratosphere | 30 | 6.8 | troposphere |
| 11 | 33.0 | stratosphere | 31 | 6.0 | troposphere |
| 12 | 30.4 | stratosphere | 32 | 5.2 | troposphere |
| 13 | 27.7 | stratosphere | 33 | 4.4 | troposphere |
| 14 | 25.1 | stratosphere | 34 | 3.6 | troposphere |
| 15 | 22.5 | stratosphere | 35 | 2.7 | troposphere |
| 16 | 21.1 | tropopause | 36 | 1.9 | troposphere |
| 17 | 19.8 | tropopause | 37 | 1.5 | troposphere |
| 18 | 18.5 | tropopause | 38 | 1.0 | troposphere |
| 19 | 17.1 | tropopause | 39 | 0.5 | troposphere |
| 20 | 15.8 | tropopause | 40 | 0.0 | surface |

The matrix $\boldsymbol{H}$ of weighting functions are computed from $\boldsymbol{x}^0$, using the radiative transfer packages 4A93 (Tournier et al., 1995; Cheruy et al., 1995; Scott and Chedin, 1981; Scott, 1974) and RTTOV (Eyre, 1991) for IASI and HIRS-TOVS, respectively. The details of the IASI and TOVS forward models will not be discussed here (a brief summary of these models and their use in the context of this information content study is provided in Prunet et al., 1998).

The observation error covariance matrix $\boldsymbol{R}$ used to specify brightness temperature data errors is the sum of 2 matrices: the instrumental error covariance matrix $\boldsymbol{E}$, and the forward model error covariance matrix $\boldsymbol{F}$. $\boldsymbol{E}$ and $\boldsymbol{F}$ are assumed to be diagonal in this study. The diagonal elements of $\boldsymbol{F}$ are all taken equal to $(0.2\ \mathrm{K})^2$ (Eyre et al., 1993). The diagonal elements of $\boldsymbol{E}$ are the squares of observation noises as specified for the instruments. These noises are given in Table 2 for some representative IASI channels (Diebel et al., 1996) and in Table 3 for HIRS-TOVS channels (Kidder and Vonder Haar, 1995, Table 4.5, p. 99).

The information content study is applied separately to the temperature profile and to the humidity profile, due to the geometrical aspects of the measure of the resolution. Such a univariate

Table 2. *Standard deviations of the radiance observation for some IASI channels (in $cm^{-1}$), expressed in noise equivalent temperature difference (K) for a reference temperature of 280 K (baseline specifications); the complete error spectrum is deduced by a linear interpolation of these values*

| Channels ($cm^{-1}$) | Brightness temperature equivalent noise (K) |
|---|---|
| 650 | 0.28 |
| 770 | 0.28 |
| 790 | 0.34 |
| 980 | 0.34 |
| 1000 | 0.28 |
| 1070 | 0.28 |
| 1080 | 0.34 |
| 1200 | 0.34 |
| 1210 | 0.28 |
| 1650 | 0.28 |
| 1660 | 0.34 |
| 2090 | 0.50 |
| 2100 | 0.50 |
| 2420 | 0.50 |
| 2430 | 0.60 |
| 2500 | 0.77 |
| 2600 | 1.10 |
| 2700 | 1.58 |
| 2760 | 1.97 |

Table 3. *Standard deviations of the radiance observation for HIRS TOVS channels (ECMWF operational configuration), expressed in noise equivalent temperature difference (K) for a reference temperature of 280 K*

| Channels ($cm^{-1}$) | Brightness temperature equivalent noise (K) |
|---|---|
| 668 | 2.77 |
| 679 | 0.74 |
| 691 | 0.55 |
| 704 | 0.31 |
| 716 | 0.18 |
| 732 | 0.18 |
| 748 | 0.14 |
| 1217 | 0.17 |
| 1364 | 0.44 |
| 1484 | 0.96 |
| 2190 | 0.10 |
| 2213 | 0.10 |
| 2240 | 0.24 |

approach assumes by definition that variables which are not retrieved are perfectly known (the effect of non-retrieved variable uncertainties on the spectrum data is not take into account in the matrix $\boldsymbol{F}$). Since each spectral radiance datum may contain information on both temperature and humidity (as well as on other atmospheric variables), a selection of the radiance spectral channels should be used to avoid overly optimistic results. The following channel selection is applied on IASI and HIRS-TOVS data. For the study of temperature, channels with significant sensitivity to water vapor and ozone content are removed from the estimation procedure. The sensitivity of a given channel $i$ to $X$ concentration ($X$ standing for humidity or ozone) is compared to the sensitivity of the same channel to temperature profile variations, by computing the following index:

$$I_{\mathrm{X}}^{i}=\sqrt{\frac{\sum_{j}\left(\dfrac{\partial T_{\mathrm{Bi}}}{\partial T_{j}}\Delta T_{j}\right)^{2}}{\sum_{j}\left(\dfrac{\partial T_{\mathrm{Bi}}}{\partial X_{j}}\Delta X_{j}\right)^{2}}}\,, \tag{21}$$

where $T_{\mathrm{Bi}}$ stands for the brightness temperature for channel $i$; $\partial T_{\mathrm{Bi}}/\partial T_j$ is the sensitivity of channel $i$ to temperature variations at level $j$, and $\partial T_{\mathrm{Bi}}/\partial X_j$ is the sensitivity of the same channel to variations in $X$ at level $j$. $\Delta T_j$ and $\Delta X_j$ are typical variations of temperature and $X$ content at level $j$. In our computations, $\Delta T_j$ is chosen equal to $1K$ at all levels, and $\Delta X_j$ is taken as 10% of the $X$ content at level $j$, both for humidity and ozone. A given channel $i$ is removed when $I_X^i$ is greater than 0.5, i.e., when the brightness temperature change due to $X$ content variation is greater than 50% of the brightness temperature change due to the temperature variation.

This selection leads to the removal of about 2500 channels sensitive to water vapor and about 100 channels sensitive to ozone in the IASI case, and 2 channels sensitive to water vapor in the HIRS-TOVS case (there is no channel sensitive to ozone, since channel 9 of HIRS-TOVS is not used in the initial configuration. For the study of humidity, the same index definition is used to remove channels with significant sensitivity to ozone content, with the same typical variation and selection thresholds. This leads to the removal of about 1150 channels in the IASI case. However, it was not possible to apply such a method to remove the channels with significant sensitivity to temperature, because the IASI and TOVS infra-red radiance measurements are essentially sensitive to temperature. The study of humidity information content is then performed without temperature sensitivity selection, which is equivalent to assuming that the temperature profile is perfectly known. This assumption is of course questionable, and will be relaxed in a further study, by introducing the impact of temperature uncertainties in the forward model error matrix $\boldsymbol{F}$.

### 3.1. *Instrument characterization*

In this section, the goal is to quantify the vertical resolution and accuracy of the state vector $\boldsymbol{x}$ derived from IASI or HIRS-TOVS data without any other information on the atmosphere. For this characterization of the instrument, we first solve the Johnson–Gilbert minimization problem for a wide range of values of the trade-off parameter $\gamma$, and compute the spread versus noise trade-off diagrams at each vertical level. Fig. 1 shows these diagrams for some typical levels for the IASI and TOVS instruments, in terms of temperature. The same diagrams in terms of humidity are plotted on Fig. 2.

The performance of the IASI instrument in terms of temperature is illustrated on Fig. 1a. The

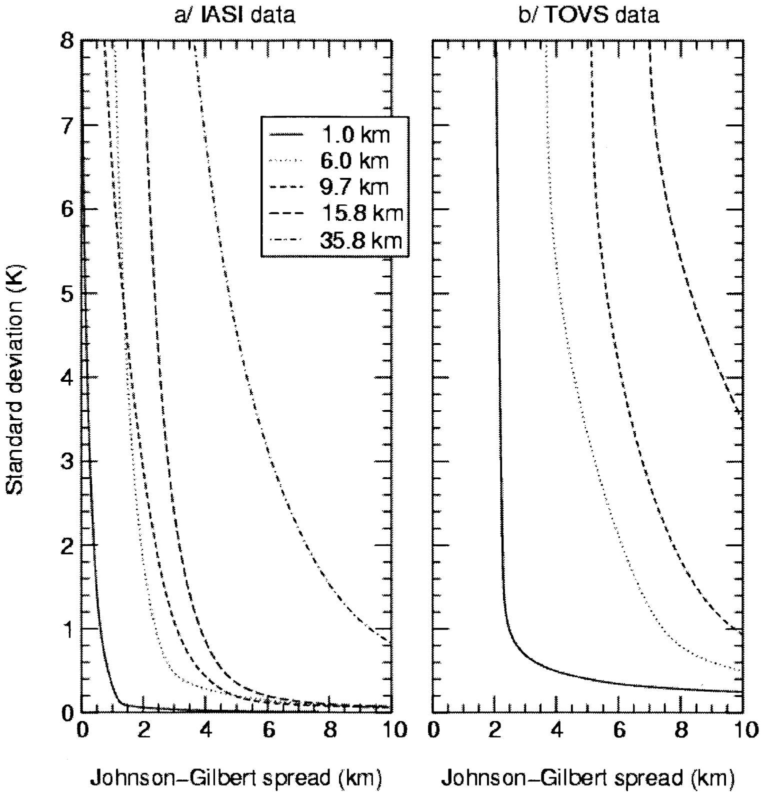


*Fig. 1.* Temperature trade-off curves presenting the resolution versus noise behaviour of the radiance data information content, for 3 tropospheric levels (1.0 km, 6.0 km, 9.7 km), 1 tropopause level (15.8 km), and 1 stratospheric level (35.8 km), when (a) IASI data only are used, and (b) TOVS data only are used. In this last case the stratospheric level is out of the plotted domain.

first three trade-off curves on Fig. 1a are associated with three tropospheric levels. The first curve indicates that the temperature at the height of 1 km can be derived from IASI data with a very good accuracy, since one can obtain a precision of 1 K with about 0.6 km of vertical resolution, or a higher precision of 0.4 K associated to a vertical resolution of 1 km. This performance is degraded for the higher tropospheric levels, with a noise of about 1 K associated with a vertical resolution of about 3 km. The performance at the tropopause for the same 1 K noise level decreases to 4 km of vertical resolution, and one obtains broader results for temperature in the stratosphere.

Fig. 1b presents comparable results for the TOVS instrument. Performances are poorer than IASI ones. The top end of the 1.0 km curve indicates that the highest resolution that can be obtained by linear combination of the weighting functions is about 2.5 km for this level, and shows that the penalty to pay is an increase of noise by a factor of about 10 compared to the noise associated with a 6-km resolution. HIRS-TOVS performances in the troposphere indicate a maximum resolution between 2.5 km and 6 km associated with noises between 1 K and 6 K, with a clear degradation from low to high troposphere. In the tropopause region, the 10 km resolution, which is about the thickness of this region, is reached with a 4 K error on the temperature estimate. The TOVS performances for the stratospheric temperature restitution (not shown) are also particularly poor. Note that this result is due to our choice of considering only the ECMWF operational system TOVS channel configuration, which does not use the stratospheric channels.

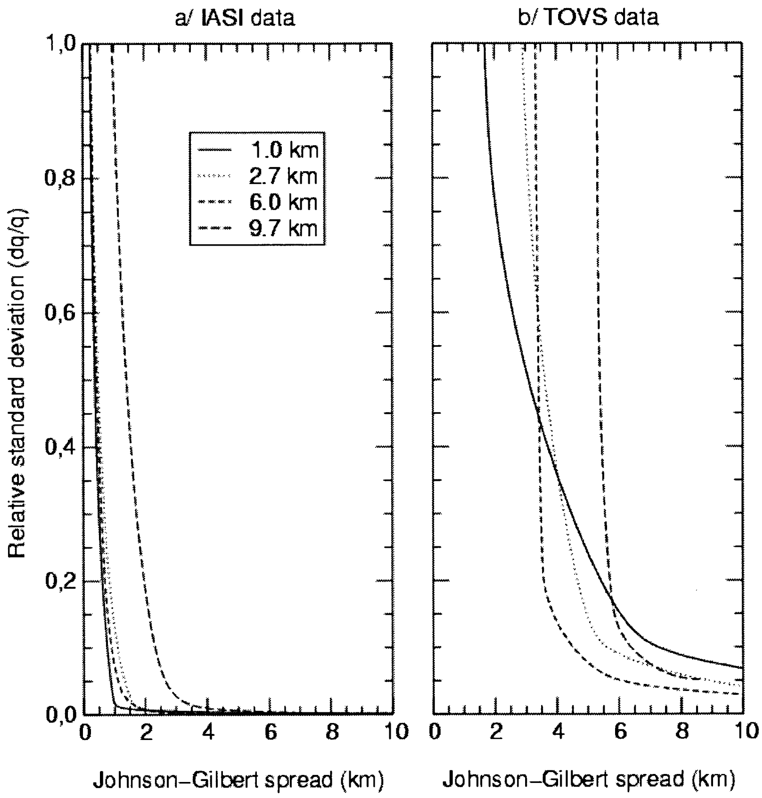


*Fig. 2.* Humidity trade-off curves presenting the resolution versus noise behavior of the radiance data information content, for 4 tropospheric levels (1.0 km, 2.7 km, 6.0 km, and 9.7 km), when (a) IASI data only are used, and (b) TOVS data only are used.

Results in terms of humidity are shown on Fig. 2, and are provided for the troposphere only, since most of the information on humidity profile deduced from the data comes from this region. For the sake of clarity of the curves, noises are expressed in terms of percentage relative to the humidity value of the level considered. This "relative error" is simply obtained by normalizing the original specific humidity error by the value of specific humidity at the level considered (this relative error is noted dq/q in the figures). A climatological humidity profile is used for this normalization, which is computed (Aires, pers. comm.) from the TIGR3 climatological database (Chevalier et al., 1997). IASI results are very good in the low and mean troposphere region (1.0 km, 2.7 km and 6.0 km curves), with a relative noise between 10% and 20% associated with a vertical resolution of about 1 km. There is a slight degradation in the upper tropospheric region (9.7 km curve) with a resolution of about 2 km associated with a noise of about 20%. TOVS data also provide humidity information in the tropospheric region, with the 20% noise level associated with resolutions between 4 and 6 km.

Results presented above indicate how the exploration of the trade-off relationship between noise and resolution allows one to map the essential properties of the information content of a given data set, and efficiently compare two instruments. More precise quantification of the information content can then be obtained by fixing a given "property" of the linear profile retrieval, for example the desired noise on the profile estimate or the minimum acceptable resolution. Such an analysis is illustrated below for IASI and TOVS. In the case of IASI data, we imposed a retrieval noise of 1 K over the whole temperature profile, and of 10% relative error on the humidity profile. In the TOVS case, the noise constraint is relaxed to 5 K on the temperature profile, and to 50% on the humidity profile. This constraint appears more reasonable, since the 1 K and 10% noise level seems to be a limit value in the TOVS case (Figs. 1, 2).

Imposing the noise on the linear retrieval turns out to fix the trade-off parameter at each level in the mollifier minimization, and then leads to a unique solution and the associated set of averaging kernels. Such a set of averaging kernels is represented on Fig. 3 in the IASI case for temperature, when the 1 K noise level is fixed. An important indication of the reliability of the averaging kernels is their miscentering, which indicates to what extent the data contain useful information on a given level. Backus and Gilbert (1968, 1970) define the "centre" of the averaging kernel as the centre of gravity:

$$c^j = \sum_k z^k (g^{jk})^2 \Big/ \sum_k (g^{jk})^2. \tag{22}$$

The variation of the centre of the averaging kernels, in the IASI and TOVS case for temperature and humidity, is shown on Fig. 4 as a function of the altitude for which the averaging kernel is computed. In terms of temperature, Fig. 4 shows useful information on the 1K-noise retrieval until the top of the stratosphere for IASI, while consistent information is only available until the top of the tropopause region (about 22-km height) in the TOVS case (note that correct temperature centres in this case would go higher if all the 19 HIRS-TOVS channels were considered). The noisy variations of the curves after the limit of relevance, for TOVS temperature, are due to negative side-lobes in the corresponding averaging kernels. In terms of humidity, both IASI and TOVS curves indicate a limit in the relevance of the retrieval around the top of the tropospheric region, which indicates the limit on the instruments ability to detect very low humidity concentrations.

The resolution for temperature and humidity profiles are presented in Figs. 5, 6. The results for temperature confirm that the vertical resolution associated with a 1 K noise level is of 1 km only in the low troposphere, and increases to 2 or 3 km in the mean and high troposphere. The resolution for TOVS temperature retrieval is broader and noisier, with a loss of information around the tropopause. In terms of humidity, good results are

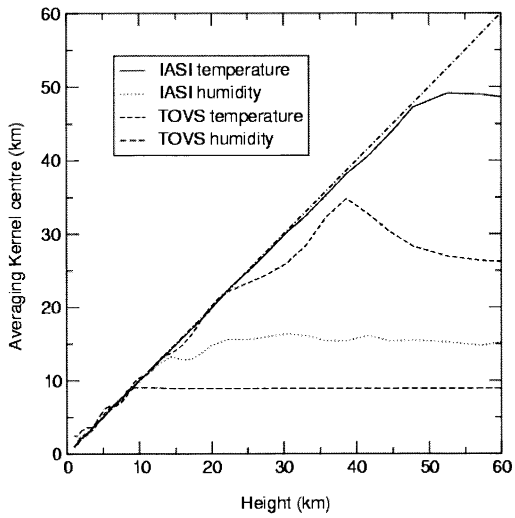


*Fig. 4.* Centre of the averaging kernels as a function of the altitude for which the averaging kernel is computed, when IASI data only are used, for temperature and humidity, and when TOVS data only are used, for temperature and humidity. The dot-dashed line indicates the ideal case where the averaging kernel centres would be at the nominal height.

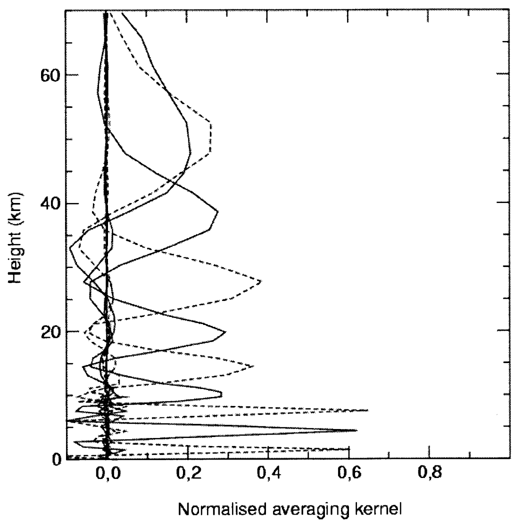


*Fig. 3.* Johnson–Gilbert averaging kernels associated with 1 K noise level in the case of temperature retrieval from IASI. 10 kernels out of the 40 (1 for each 4 levels) are plotted.

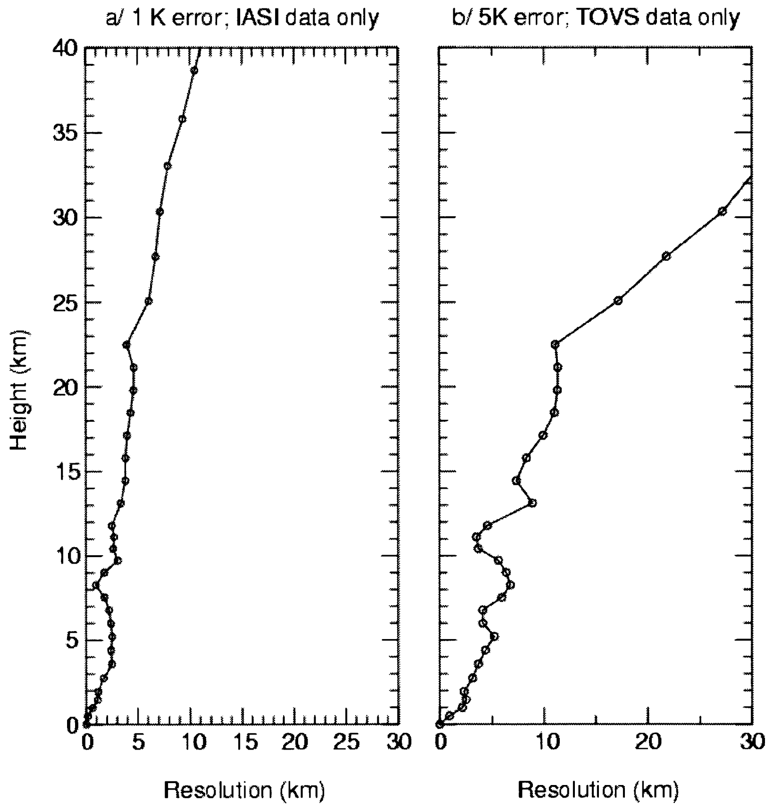


*Fig. 5.* Vertical resolution of the temperature retrieval computed for the averaging kernels using the Johnson–Gilbert spread formulation when (a) IASI data are used only, and (b) TOVS data are used only.

obtained for IASI, with 1 or 2 km resolution associated with 10% relative error below 9 km height in the IASI case, while the TOVS data instrument gives a resolution between 4 and 6 km in the troposphere, associated with a 50% noise level. Note finally the noisy behavior of the resolution curves (Fig. 6) and of the averaging kernel centre positions (Fig. 4) for humidity near the surface in the TOVS case, which suggests a lower detection limit for the humidity near the surface, a feature which is not present in the IASI results.

### 3.2. *Adding a priori information*

We use below the MR approach with the inclusion of prior statistics as extra measurements to investigate the information content of the IASI data in the context of two particular problems: the "climatological case" which includes the minimal climatological prior information; and the "forecast case" which includes background information coming from a given numerical weather prediction (NWP) system. A priori information associated with these two problems is detailed below. The MR formulation allows us to analyse the information content of the classical BLUE solution at the limit $\gamma = 0$, and to investigate how the precision of this solution could be improved by a smoothing of the solution (i.e., a degradation of the vertical resolution in the sense of the Johnson–Gilbert spread), using the trade-off curve.

3.2.1. *Climatological case.* The error covariance matrix associated with the climatological knowledge of the atmosphere behavior (hereafter named $\boldsymbol{B}_c$), which is used as prior information in the context of the climatological case, was computed

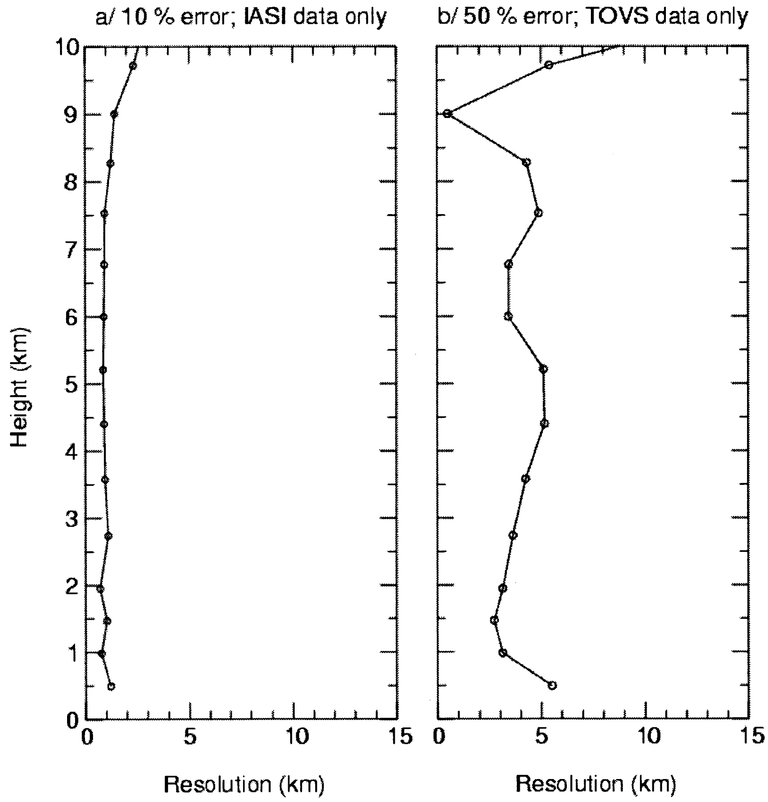


*Fig. 6.* Same as Fig. 6 but for the humidity retrieval.

empirically (Aires, pers. comm.) from the TIGR2 database (Chedin et al., 1985; Achard, 1991; Escobar, 1993) for temperature, and from the TIGR3 database (Chevalier et al., 1997) for humidity. Associated standard deviations are shown in Table 4. Note that inter-level correlations for temperature and humidity structures (not shown) are important constraints for the inversion problem. These statistics show relatively high noise, and in the case of a realistic inversion, more accurate climatological statistics based, for example, on air mass selection should be commonly available. In terms of temperature, the $\boldsymbol{B}_{\mathrm{c}}$ matrix was directly computed over the 40 atmospheric levels given in Table 1, and the associated matrix $\boldsymbol{H}_{\mathrm{c}}$ of weighting functions is the $\boldsymbol{I}_n$ matrix. However, useful statistics on the TIGR humidity profiles are available only for the lowest 23 levels (levels 17 to 39 in Table 1). Then in terms of humidity, $\boldsymbol{B}_{\mathrm{c}}$ is a $23 \times 23$ covariance matrix, and the associated matrix $\boldsymbol{H}_{\mathrm{c}}$ of weighting functions is the $\boldsymbol{I}_n$ matrix where the diagonal terms are forced to zero for levels 1 to 16, which simply means that no prior information is available for these levels (i.e., above the tropopause).

We may compute trade-off curves for the radiance data with prior information, and for the prior statistics alone, which may be compared to the trade-off curves for the radiances alone computed in Subsection 3.1. All three curves are shown for temperature on Fig. 7 for some typical levels. The trade-off curve for prior information alone just means that we may derive prior statistics with broader resolution which will have smaller values of variance. When we make use of both the measurements and the prior information we obtain a major improvement in the noise, regarding the IASI radiances alone, in regions of (relative) low spread. Note that on the graphs of Fig. 7, the spread scale does not start at zero, but at 0.5 km,

Table 4. *Standard deviations of the climatological statistics for temperature (K) and humidity (in relative error, obtained by dividing the standard deviation by the mean climatological profile value at the considered level); no useful statistics was available for the 16 first humidity levels (see text)*

| Levels | Temperature standard deviation (K) | Humidity standard deviation ($dq/q$) | Levels | Temperature standard deviation (K) | Humidity standard deviation ($dq/q$) |
|---|---|---|---|---|---|
| 1 | 14.7 | | 21 | 9.5 | 71.6 |
| 2 | 12.3 | | 22 | 8.9 | 74.3 |
| 3 | 10.5 | | 23 | 9.3 | 79.4 |
| 4 | 10.2 | | 24 | 9.0 | 81.8 |
| 5 | 11.3 | | 25 | 9.4 | 84.2 |
| 6 | 13.9 | | 26 | 9.4 | 85.4 |
| 7 | 14.1 | | 27 | 9.9 | 87.3 |
| 8 | 14.6 | | 28 | 10.2 | 87.1 |
| 9 | 14.6 | | 29 | 10.5 | 86.2 |
| 10 | 15.1 | | 30 | 10.8 | 84.5 |
| 11 | 14.9 | | 31 | 11.1 | 82.4 |
| 12 | 14.7 | | 32 | 11.2 | 76.9 |
| 13 | 13.9 | | 33 | 11.4 | 74.5 |
| 14 | 13.8 | | 34 | 11.7 | 73.2 |
| 15 | 13.1 | | 35 | 12.1 | 71.5 |
| 16 | 12.6 | | 36 | 12.8 | 69.7 |
| 17 | 12.1 | 57.8 | 37 | 13.2 | 69.2 |
| 18 | 11.7 | 60.7 | 38 | 14.0 | 68.7 |
| 19 | 11.2 | 63.6 | 39 | 15.2 | 68.6 |
| 20 | 10.5 | 67.7 | 40 | 16.8 | – |

which is the vertical discretisation of the lower levels. At 1 km height, a useful improvement around a spread level of 1 km can be noticed (Fig. 7a). Figs. 7a–c show that a noise lower than or equal to 1 K is obtained even without any smoothing of the profile, in the troposphere and tropopause region. Good results are also obtained in the stratosphere (Fig. 7d). In this case however, the prior information may be unrealistically good in particular for the low spreads. Indeed, the measured profiles of the TIGR climatology database are frequently extrapolated with climatological models in the stratosphere, which implies little variability at small spatial scales at these altitudes. Nevertheless, These results indicate a useful improvement in the ability to retrieve temperature profiles using the IASI radiances when they are used with such climatological information. This suggests that the 1 K noise/1 km resolution specification on temperature retrieval would be easily reached, at least in the troposphere, from IASI radiance inversion.

Similar calculations have been carried out for humidity, but the conclusions significantly differ. The trade-off curves computed for several tropospheric levels using both the measurements and the a priori information (not shown), indicate no difference with those computed with the radiances alone in the useful noise versus spread regions. This is due to the very low quality of the climatological humidity statistics (Table 4) which have an effective impact on the information content only in the region of the trade-off curves where the noise is relatively high (larger than 50% of relative standard deviation).

The MR method performed for $\gamma = 0$ for temperature, when both measurements and a priori information are used, gives the BLUE estimate of the temperature profile, which realizes the linearly optimal use of the available information, given our profile vertical discretization. One may compute the noise associated with this estimate, and with its parts coming from the measurements and the statistics, using the $\boldsymbol{A}$, $\boldsymbol{A}_m$ and $\boldsymbol{A}_b$ matrices of eq. (20), respectively. Diagonal terms of these matrices are shown on Fig. 8, and represent the standard deviation noise associated with each discretized level. The noise coming from the prior

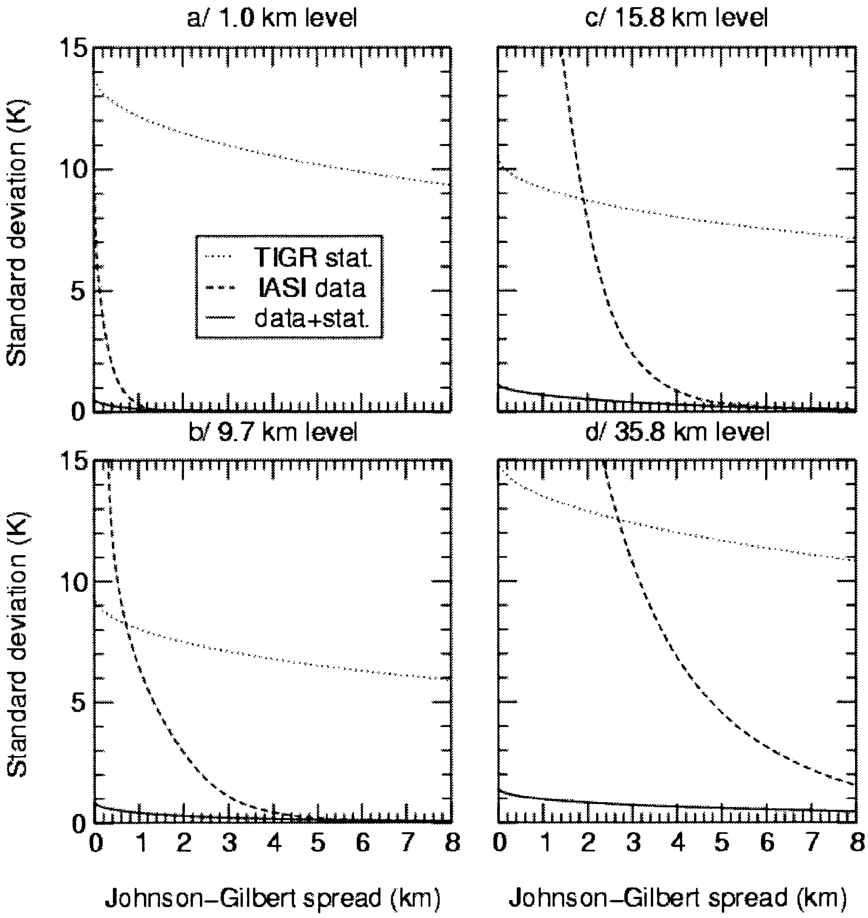


*Fig. 7.* Temperature trade-off curves for prior statistics alone (dotted line) for the IASI radiance data alone (dashed line), and for the radiance data with prior statistics (solid line): (a) at 1.0 km height (low troposphere), (b) at 9.7 km height (high troposphere), (c) at 15.8 km height (tropopause), and (d) at 35.8 km height (stratosphere).

information is also called the smoothing error (Rodgers, 1990) and results from those components of the profile that cannot be recovered by the radiance inversion. The total noise shows errors of around 1 K up to the top of the tropopause, and reasonable errors in the stratosphere. This confirms our previous results.

*3.2.2. Forecast case.* The error covariance matrix used to illustrate the problem of IASI data utilization for NWP (hereafter named $\boldsymbol{B}_f$) is determined by averaging the non-separable background error covariance matrices used by the ECMWF NWP system (Rabier and Mac Nally, 1993), and is the same as that used by Prunet et al. (1998) in their IASI information content study. The diagonal terms of $\boldsymbol{B}_f$ are shown in Table 6. The correlation structures for temperature and humidity may be found in Prunet et al. (1998). The $\boldsymbol{B}_f$ matrix is only available over the 31 levels of the ECMWF numerical model (Table 5), which have no exact correspondance with the 40 levels of our discretization. The pertinent problem, in the context of the radiance utilization for NWP, is to retrieve the atmospheric state at the discretization of the forecast numerical model, to obtain an analysis of the atmospheric state which will be used as an initial condition for this model. In this section, we modified our initial discretization of the atmosphere to provide an information content analysis

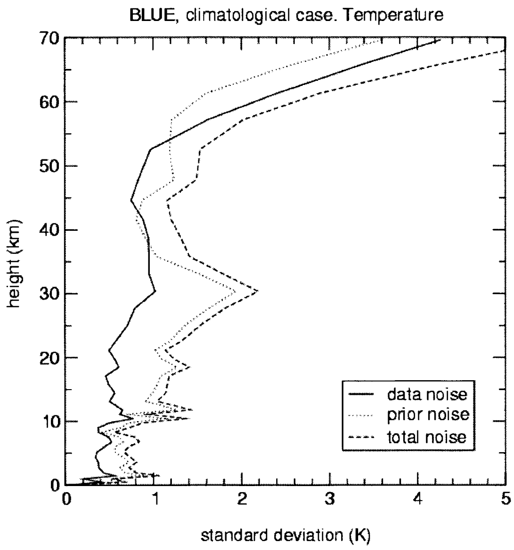


*Fig. 8.* Error standard deviations of the retrieved temperature profile in the BLUE case (dashed line), with the proportions coming from the data (solid line) and from the prior statistics (dotted line).

which answers this problem. The results presented below are computed for a temperature/humidity profile discretized over the 31 levels given in Table 5. The separation of the atmospheric column into troposphere, tropopause and stratosphere region is maintained, and is also indicated in Table 5 for this new discretization (in this case, there is no level in the "upper layers" defined in Table 1).

If such high quality prior information is available, one can obtain considerably better results as shown in Fig. 9 in terms of temperature, and in Fig. 10 in terms of humidity. Below the 30 km height where the numerical forecast model provides information, the impact of this information on IASI information content is determinent, and leads obtaining a noise lower than 1 K on the temperature retrieval at all levels, even when no smoothing is performed. No result for the stratospheric region is presented in Fig. 9, since the new discretization has only two very thick layers in this region, which does not allow significant results to be obtained on the trade-off curves for the stratosphere. The results for humidity are also improved. In the troposphere, the forecast model prior information allows a reduction in the noise of the humidity retrieval in the regions of the trade-off diagram where the resolution is lower than 3 km. A noise of around 10% is reached, when $\gamma = 0$, in the low and mean troposphere (Fig. 10a–c), while a noise level of 20% is found in the top of the troposphere (Fig. 10d).

The noise associated with the BLUE estimate, and its parts coming from the measurements and the prior information, are shown on Fig. 11 for temperature and humidity, and are compared with the initial a priori noise associated to the prior

Table 5. *Discretized vertical levels on which the atmospheric state is represented in the ECMWF forecast model, and the corresponding vertical region*

| Levels | Height (km) | Region | Levels | Height (km) | Region |
|---|---|---|---|---|---|
| 1 | 31.1 | stratosphere | 17 | 6.2 | troposphere |
| 2 | 23.8 | stratosphere | 18 | 5.6 | troposphere |
| 3 | 20.6 | tropopause | 19 | 5.0 | troposphere |
| 4 | 18.4 | tropopause | 20 | 4.4 | troposphere |
| 5 | 16.8 | tropopause | 21 | 3.8 | troposphere |
| 6 | 15.5 | tropopause | 22 | 3.2 | troposphere |
| 7 | 14.4 | tropopause | 23 | 2.7 | troposphere |
| 8 | 13.4 | tropopause | 24 | 2.2 | troposphere |
| 9 | 12.4 | tropopause | 25 | 1.8 | troposphere |
| 10 | 11.5 | tropopause | 26 | 1.3 | troposphere |
| 11 | 10.7 | troposphere | 27 | 0.96 | troposphere |
| 12 | 9.9 | troposphere | 28 | 0.63 | troposphere |
| 13 | 9.1 | troposphere | 29 | 0.35 | troposphere |
| 14 | 8.3 | troposphere | 30 | 0.15 | troposphere |
| 15 | 7.6 | troposphere | 31 | 0.03 | troposphere |
| 16 | 6.9 | troposphere | 32 | 0.00 | surface |

Table 6. *Standard deviations of the forecast error for temperature (K) and humidity (in relative error)*

| Levels | Temperature standard deviation (K) | Humidity standard deviation ($dq/q$) | Levels | Temperature standard deviation (K) | Humidity standard deviation ($dq/q$) |
|---|---|---|---|---|---|
| 1 | 1.5 | 0.0003 | 17 | 0.95 | 1.6 |
| 2 | 1.1 | 0.004 | 18 | 0.93 | 1.3 |
| 3 | 1.0 | 0.006 | 19 | 0.91 | 1.1 |
| 4 | 0.96 | 0.02 | 20 | 0.91 | 1.0 |
| 5 | 0.94 | 0.07 | 21 | 0.91 | 0.90 |
| 6 | 0.88 | 0.19 | 22 | 0.91 | 1.0 |
| 7 | 0.91 | 0.44 | 23 | 0.94 | 1.5 |
| 8 | 0.95 | 1.0 | 24 | 0.94 | 1.4 |
| 9 | 1.0 | 1.8 | 25 | 0.90 | 0.85 |
| 10 | 1.1 | 7.2 | 26 | 0.88 | 0.43 |
| 11 | 1.1 | 2.8 | 27 | 0.88 | 0.26 |
| 12 | 0.96 | 11.7 | 28 | 0.84 | 0.21 |
| 13 | 0.90 | 2.1 | 29 | 0.72 | 0.17 |
| 14 | 0.91 | 1.6 | 30 | 0.60 | 0.15 |
| 15 | 0.94 | 2.9 | 31 | 0.53 | 0.14 |
| 16 | 0.97 | 1.6 | 32 | 2.0 | – |

statistics alone (diagonal terms of the $\boldsymbol{B}_f$ matrix), allowing an estimation of the contribution of the data to the analysis. For both the temperature and humidity BLUE estimate, the contribution of statistical information to the analysis of the atmospheric state is obviously important. For temperature, the contribution of the data is significant at all levels, leading to an improvement by a factor of 2 on the noise estimate, compared to a priori statistics. In terms of humidity, the contribution of the data is slight below 1 km, and becomes important for higher levels, allowing an improvement by a factor of 3 or 4 on the noise estimate, compared to a priori statistics.

Note that these results are in good agreement with results of a comparable study performed by Prunet et al. (1998) and complete that study by adding the notion of resolution versus noise performances of the IASI radiance data.

The impact of adding a priori information on the performance of IASI data information content is summarized on Fig. 12, in the case where 1 K noise for temperature and 10% relative noise for humidity are specified. Fig. 12 shows for each level of the discretized temperature and humidity profiles, the associated vertical resolution for the different configurations examined above. For temperature, only configurations with IASI data alone and with IASI data plus climatological information are considered, since results which use NWP model information give a perfect resolution with noise always better than 1 K. For the humidity case, configuration with IASI data plus climatological information gives similar results than that with IASI data only, and therefore is not shown.

These figures summarize our above results on IASI data performance. In terms of temperature, the 1 K versus 1 km performance can not be achieved using the IASI data only, since it leads to a vertical resolution between 2 and 3 km in the troposphere for the 1 K noise level. However, the addition of a "minimal" climatological information strongly improves the results, and leads to a vertical resolution equal to or better than 1 km in the whole troposphere, and between 1 and 2 km in the tropopause region. Since this a priori information is always available, such performances are accessible with the IASI instrument. For humidity, results with IASI data only are very promising, with a vertical resolution between 1 and 2 km in the troposphere associated with the 10% noise level, and the addition of the low quality climatological prior information has no impact on such good performances. However, the combination of these data with high quality humidity information provided by a NWP model leads to a significant improvement of the resolution for the same noise level, particularly in the low troposphere.

Fig. 12 also illustrates an empirical way to

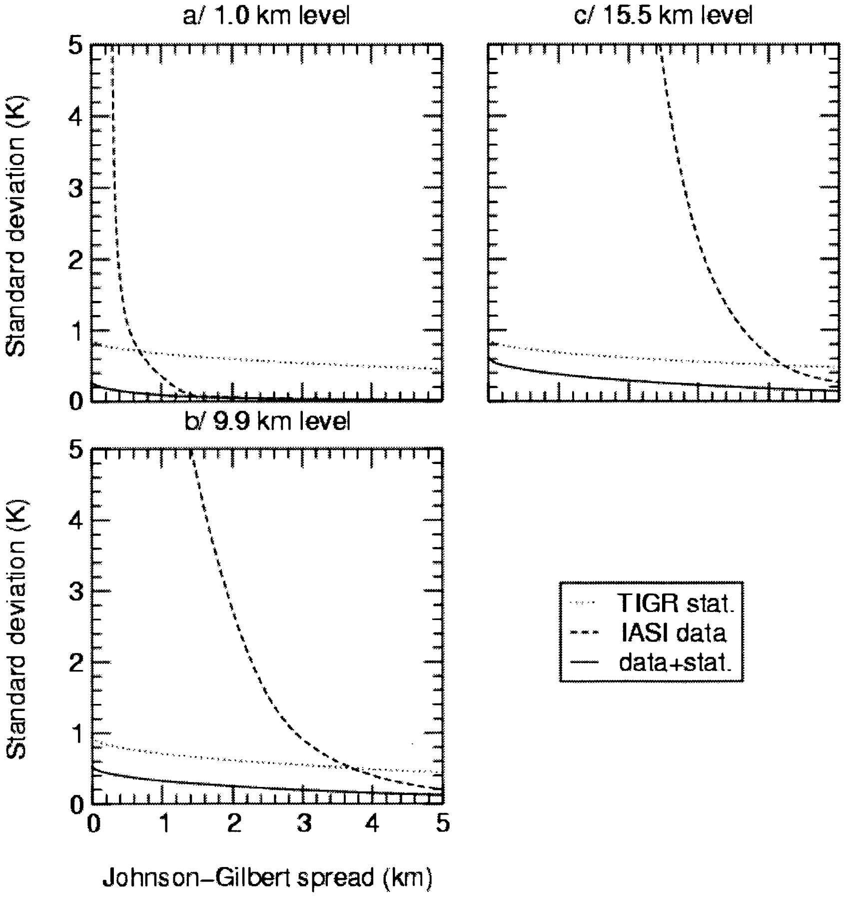


*Fig. 9.* Temperature trade-off curves for the forecast prior statistics alone (dotted line), for the IASI radiance data alone (dashed line), and for the radiance data with forecast prior statistics (solid line): (a) at 1.0 km height (low troposphere), (b) at 9.9 km height (high troposphere), and (c) at 15.5 km height (tropopause).

deduce an optimal vertical discretization of the atmospheric column for a temperature/humidity retrieval, depending on the particular configuration. Indeed, as illustrated for the temperature case with IASI data alone (Fig. 12a), it is possible to use these results to derive the relevant independent layers which give an optimized vertical discretization, given the fixed configuration (in the example, temperature retrieval from IASI data alone) and the desired noise figure associated with the retrieval (in the example, 1 K standard deviation at all vertical levels). The bold vertical resolution bars on Fig. 12a suggest the 11 or 12 vertical layers (below 50 km height) on which the temperature profile could be discretized in this case (if the initial discretization of the atmospheric profile chosen to perform the information content analysis is sufficiently accurate, such optimal layers can be deduced without ambiguity). The same approach allows one to deduce, from the other results plotted in Fig. 12, about 30 layers for the temperature retrieval from the IASI data plus climatological information (given the 1 K noise level), about 6 tropospheric layers for the humidity retrieval from IASI data alone, and about 15 tropospheric layers if NWP model information is added, given the 10% relative noise level. This approach may easily be applied to any desired configuration, and can be seen as a comprehensive and objective first step to deal with the problem

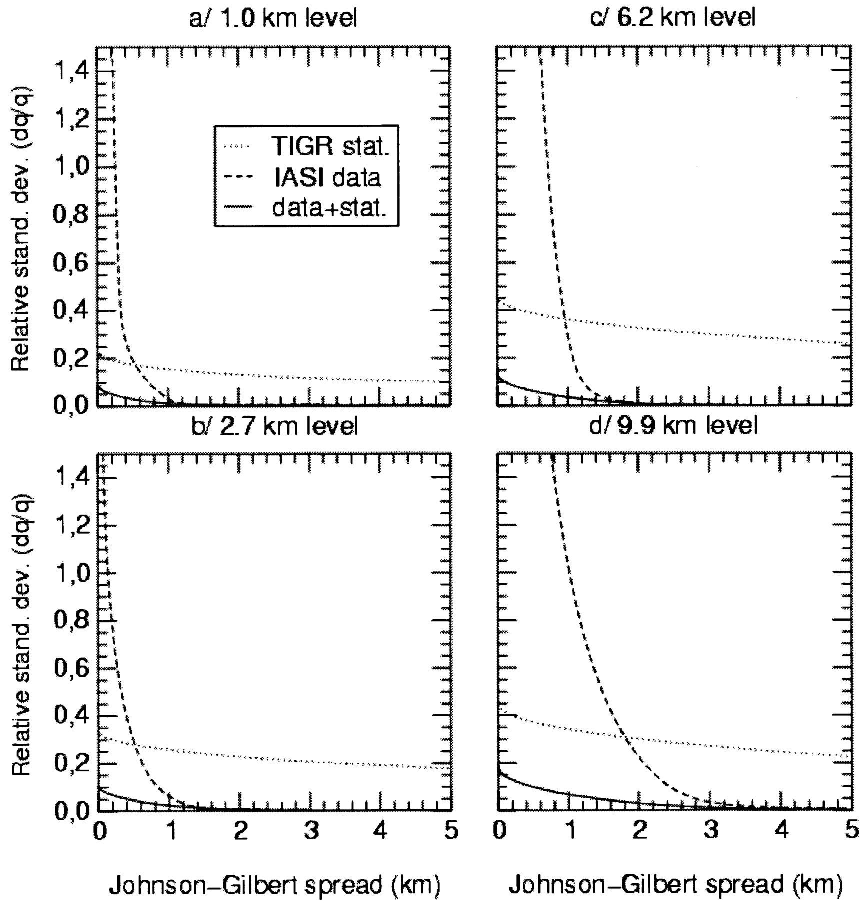


*Fig. 10.* Humidity trade-off curves for the forecast prior statistics alone (dotted line), for the IASI radiance data alone (dashed line), and for the radiance data with forecast prior statistics (solid line) at 4 tropospheric levels: (a) at 1.0 km height, (b) at 2.7 km height, (c) at 6.2 km height, and (d) at 9.9 km height.

of finding appropriate vertical discretizations in any retrieval problem.

## 4. Conclusions

We used in this work two methods of regularization of the ill-posed linear inverse problem for the study of the performance of the IASI and HIRS-TOVS infra-red sounders. The Tikhonov regularization (TR) is based on the addition of independent information about the atmospheric state to reduce the noise on the solution, while the mollifier regularization (MR) explores what can be said from the radiance data only by allowing a degradation of the vertical resolution of the retrieved profile. The formal equivalence between these two methods was used to propose a complete analysis of the information content of the radiance data in terms of potential accuracy and vertical resolution associated with the temperature/humidity profile derived from these data.

The MR approach was first applied to the analysis of the information content of IASI and HIRS-TOVS radiance data without any other independent information. This analysis showed that the estimation of the temperature and humidity profile is considerably improved when IASI measurements are used instead of the HIRS-TOVS

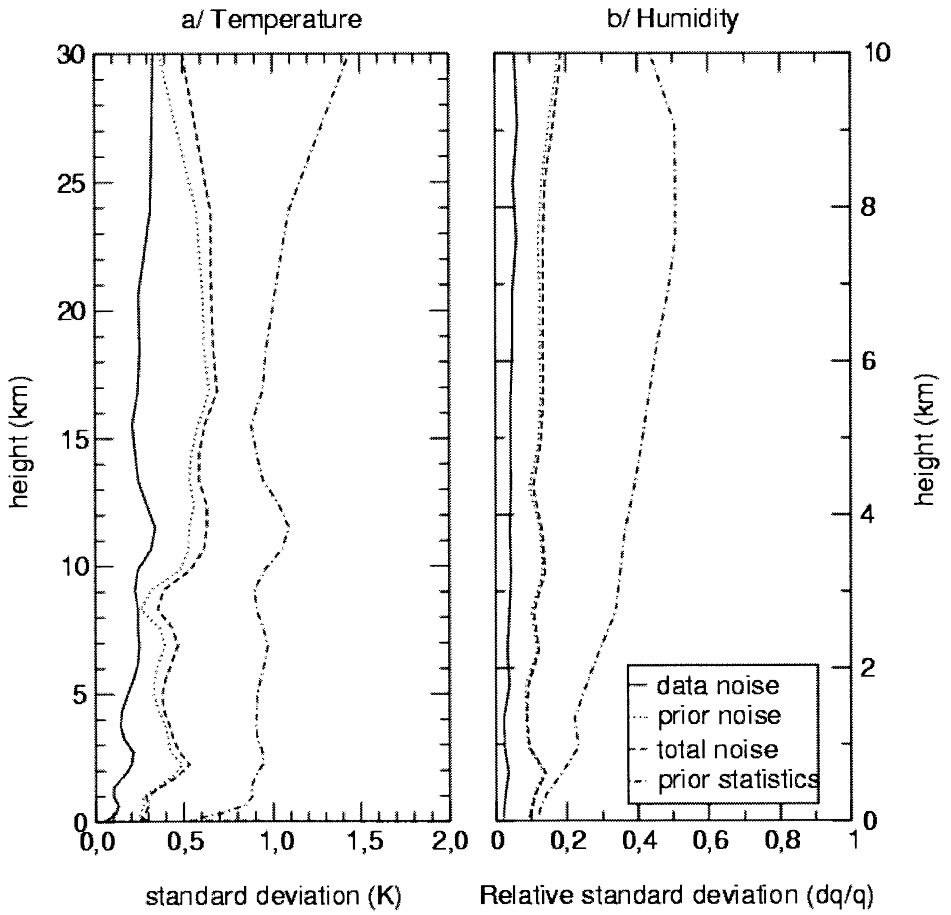


*Fig. 11.* Error standard deviations of the retrieved profile in the BLUE case (dashed line), and the proportions coming from the data (solid line) and from the prior statistics (dotted line). The standard deviation noise associated with the a priori forecast statistics (dotted-dashed line) is also given. (a) temperature retrieval, and (b) humidity retrieval.

data currently used for operational applications. The analysis of the behaviour of resolution versus noise suggests that the performance of the IASI measurements is close to 1 K accuracy at 2 km resolution for temperature in the troposphere, and between 10 and 20% relative error at 1 km resolution for humidity in the troposphere. The same analysis shows broader results for HIRS-TOVS, for which the useful temperature information is limited to the troposphere, with a maximum resolution of 2 km associated with noise between 1 and 5 K, and for which humidity information in the troposphere indicates 20% relative error associated with a resolution between 4 and 6 km. The above IASI performances may also be compared with comparable studies on other new generation souding instruments (e.g., Huang et al., 1992; Rodgers, 1998).

Then TR and MR equivalence was used to study the behavior of the IASI information content when independent a priori information is available under the form of statistics on the atmospheric state. Two cases were examined. First, the "climatological case" is considered, when minimal climatological prior information on temperature and humidity profiles are added to the IASI data to perform the analysis of the atmospheric state. In terms of temperature, we obtained a major

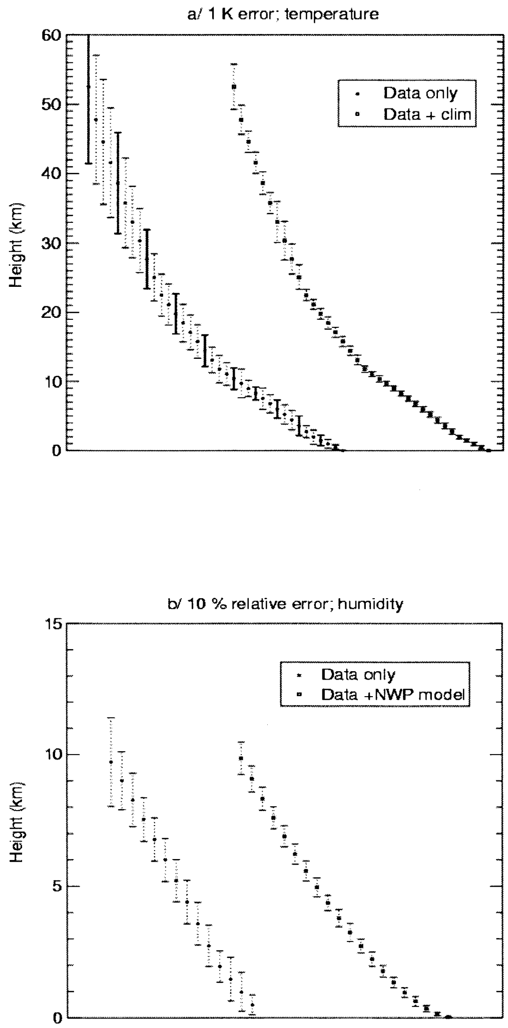


*Fig. 12.* Schematic representation of the vertical resolution as a function of height: (a) temperature, when IASI data alone are used, and when IASI data are used with climatological prior information; (b) humidity, when IASI data alone are used, and when IASI data are used with NWP model prior information. The bold bars illustrate the vertical discretization which can be deduced from such scheme for the inversion of temperature profiles from IASI data alone. The horizontal dimension is used to allow distinction of model levels.

improvement of the profile retrieval accuracy in the region of relatively good resolution, and results indicate performances better than 1 K noise/1 km resolution in the troposphere, and of this order of magnitude in the troposphere and stratosphere. In terms of humidity however, the climatological statistics are poor regarding the IASI instrument performances, and no significant improvement was provided by the use of these statistics. Second, the "forecast case" was considered, when a priori statistics are provided by a numerical weather prediction system. If such a priori information is available with IASI data, then the analysis of the atmospheric state is considerably better both for temperature and humidity, and shows that the detection of temperature structures at a very good vertical resolution with a noise better than 1 K, and of humidity structures at a good accuracy with a vertical resolution of 1 km in the troposphere, may be achievable in the context of the assimilation of IASI data in NWP systems.

Finally, the above results are used to propose a possible way to objectively determine a vertical discretization of the atmospheric column adapted to any given temperature/humidity profile retrieval problem.

It is worth stressing that the results presented above are conditioned by the limitations of the study, essentially the linear hypothesis, and the univariate approach of the information content analysis which probably give optimistic results in terms of humidity. However, this case study clearly points out the improved performances of the next generation of infra-red sounders such as IASI, and the potential gain one can obtain from these new observing systems. Furthermore, such an analysis allows to illustrate the importance of the introduction of our a priori knowledge on the atmosphere for the study of information content, and the necessity of a good understanding of how this information is used by the inversion procedure, for a correct interpretation and an efficient use of data potentialities.

## 5. Aknowledgments

We thank F. Aires and the ARA team from the Laboratoire de Meteorologie Dynamique for providing us with TIGR data. F. Rabier and C. Camy-Peyret are warmly aknowledged for helpful comments and useful discussions. We also thank two anonymous rewievers for their comments. This research was performed in the framework of the ISSWG activities under the auspice of EUMETSAT and CNES.

## REFERENCES


Achard, V. 1991. *Trois probleµes clés de l'analyse tridimentionnelle de la structure thermodynamique de l'atmosphepe par satellite: mesure du contenu en ozone, classification des masses d'air, modélisation hyperrapide du transfert radiatif.* PhD thesis, Université Pierre et Marie Curie, Paris, France.

Backus, G. and Gilbert, F. 1968. The resolving power of gross earth data, Geophys. *J. Roy. Astron. Soc.* **16**, 169–205.

Backus, G. and Gilbert, F. 1970. Uniqueness in the inversion of inaccurate gross earth data. *Phil. Trans. Roy. Soc. London* **A266**, 123–192.

Chahine, M. T. 1991. AIRS: the atmospheric infrared sounder. *Optics and Photonics News* **2**, 10, 25.

Chedin, A., Scott, N., Wahiche, C. and Moulinier, P. 1985. The improved initialisation inversion method: a high resolution physical method for temperature retrievals from Tiros-N series. *J. Clim. Appl. Meteor.* **24**, 128–143.

Cheruy, F., Scott, N. A., Armante, R., Tournier, B. and Chedin, A. 1995. Contribution to the development of radiative transfer models for high spectral resolution observations in the infrared. *J. Quant. Spectrosc. Radiat. Transfer* **53**, 597–611.

Chevalier, F., Cheruy, F., Scott, N. A. and Chedin, A. 1997. *A fast and accurate neural network-based computation of longwave radiative budget in clear and in cloudy situations.* IGLS meeting, Austria, 1997.

Conrath, B. J. 1972. Vertical resolution of temperature profiles obtained from remote radiation measurements. *J. Atmos. Sci.* **29**, 1262–1271.

Diebel, D., Cayla, F. and Phulpin, T. 1996. Mission rationale and requirements, CNES/EUMETSAT Report IA-SM-0000-10-CNE/EUM, Issue 3.

Escobar, J. 1993. *Base de données pour la restitution de parameτres atmosphériques à l'échelle globale; étude sur l'inversion par réseaux de neurones des données des sondeurs verticaux atmosphériques satellitaires présents et à venir.* PhD thesis, Université Denis Diderot.

Eyre, J. R. 1991. *A fast radiative transfer model for satellite sounding systems.* ECMWF Tech. Memo. 176 (available from ECMWF, Shinfield Park, Reading, UK).

Eyre, J. R., Kelly, G. A., McNally, A. P., Anderson, E. and Persson, A. 1993. Assimilation of TOVS radiance information through one-dimensional variational analysis. *Q. J. R. Meteorol. Soc.* **119**, 1427–1463.

Hansen, C. 1998. *Rank-deficient and discrete ill-posed problems: numerical aspects of linear inversion.* Siam Monographs on Mathematical Modelling and Computation.

Huang, H.-L., Smith, W. L. and Woolf, H. M. 1992. Vertical resolution and accuracy of atmospheric sounding spectrometers. *J. Appl. Meteor.* **31**, 265–274.

Ide, K., Courtier, P., Ghil, M. and Lorenc, A. C. 1997. Unified notation for data assimilation: operational, sequential and variational. *J. Meteor. Soc. Japan* **75**, 181–189.

Johnson, L. E. and Gilbert, F. 1972. Inversion and inference for teleseismic data. *Method in Computational Physics* **12** (B. A. Bolt, ed.). Academic Press, New York, pp. 231–266.

Kaplan, L. D. 1959. Inference of atmospheric structure from remote radiation measurements. *J. Opt. Soc. Am.* **49**, 1004–1007.

Kaplan, L. D., Chahine, M. T., Susskind, J. and Searl, J. E. 1977. Spectral band passes for a high precision satellite sounder. *Appl. Opt.* **16**, 322–325.

Kidder, S. Q. and Vonder Haar, T. H. 1995, *Satellite meteorology. An introduction.* Academic Press, New York.

Lorenc, A. C. 1986. Analysis methods for numerical weather prediction. *Quart. J. R. Met. Soc.* **112**, 1177–1194.

Menke, W. 1984. Geophysical data analysis, *Discrete inverse theory*. Academic Press, New York, 289 p.

Ory, J. and Pratt, G. 1994. Are our parameter estimators biased? The significance of finite-difference regularization operators. *Inverse Problems* **11**, 397–424.

Purser, R. J. and Huang, H.-L. 1993. Estimating effective data density in a satellite retrieval or an objective analysis. *J. Appl. Meteor.* **32**, 1092–1106.

Press, W. H., Teukolsky, S. A., Vetterling, W. T. and Flannery, B. P. 1992. Numerical recipies in FORTRAN, 2nd edition. Cambridge University Press, Cambridge, 935 p.

Prunet, P, Thépaut, J.-N. and Cassé, V. 1998. The information content of clear sky IASI radiances and their potential for numerical weather prediction. *Q. J. R. Meteorol. Soc.* **124**, 211–241.

Rabier, F., Klinker, E., Courtier, P. and Hollingsworth, A. 1996. Sensitivity of forecast errors to initial conditions, *Q. J. R. Meteorol. Soc.* **122**, 121–150.

Rabier, F., McNally, A., Andersson, E., Courtier, P., Unden, P., Eyre, J., Hollingsworth, A. and Bouttier, F. 1998. The ECMWF implementation of three-dimensional variation assimilation (3D-Var). II: Structure functions. *QJRMS* **124**, 1809–1829.

Rochard, G. 1979. *Etude numérique de la restitution du profil vertical des température dans l'atmosphepe à partir de mesures satellitaire.* EERM Technical notes 12 and 20 (available from Météo-France).

Rodgers, C. D. 1976a. Retrieval of atmospheric temperature and composition from remote measurements of thermal radiation. *Rev. Geophys. and Space Phys.* **14**, 609–624.

Rodgers, C. D. 1976b. The vertical resolution of remotely sounded temperature profiles with a priori statistics. *J. Atmos. Sci.* **33**, 707–709.

Rodgers, C. D. 1990. Characterization and error analysis of profiles retrieved from remote sounding measurements. *J. Geophys. Res.* **95**, 5587–5595.

Rodgers, C. D. 1998. Information content and optimisation of high spectral resolution remote measurements. *Adv. Space Res.* **21**, 1421–1424.

Rodi, W. L. 1991. Smoothest models and Backus–Gilbert inference. In: *Notes on inversion.* W. L. Rodi and J. G. Berryman, Founding Members Technical report, ERL, Massachusetts Institute of Technology, pp. 75–121.

Scott, N. A. 1974. A direct method of computation of the transmission function of an inhomogeneous gaseous medium. Part I: description of the method and influence of various factors. *J. Quant. Spectrosc. Radiat. Transfer* **14**, 691–707.

Scott, N. A. and Chedin, A. 1981. A fast line-by-line method for atmospheric absorption computations: the automatized atmospheric absorption atlas. *J. Appl. Meteor.* **20**, 802–812.

Shannon, C. 1949. Communication in the presence of noise. *Proc. I. C. E.* **37**, 10–21.

Smith, W. L. and Woolf, H. M. 1976. The use of eigenvectors of statistical covariance matrix for interpreting satellite sounding radiometer observation. *J. Atmos. Sci.* **33**, 1127–1140.

Smith, W. L., Woolf, H. M., Hayden, C. M., Wark, D. Q. and McMillin, L. M. 1979. The Tiros-N operational vertical sounder. *Bull. Amer. Meteorol. Soc.* **60**, 1177–1187.

Tarantola, A. and Valette, B. 1982. Generalised nonlinear inverse problems solved using the least square criterium. *Rev. Geophys. and Space Phys.* **20**, 219–232.

Thépaut, J.-N. and Moll, P. 1990. Variational inversion of simulated TOVS radiances using the adjoint technique. *Q. J. R. Meteorol. Soc.* **116**, 1425–1448.

Thompson, O. E. 1982. HIRS-AMTS satellite sounding system test — theorical and empirical vertical resolving power. *J. Appl. Meteor.* **21**, 1550–1561.

Tikhonov, A. N. 1963. On the solution of incorrectly stated problems and a method of regularization. *Dokl. Acad. Nauk. SSSR* **151**, 501.

Tournier, B., Armante, R. and Scott, N. 1995. STRANSAC93-4A93. *Développement et validation des nouvelles versions de code de transfert radiatif pour applications au projet IASI*. LMD Tech. Note 201.

Twomey, S. 1963. On the numerical solution of Fredholm integral equations of the first kind by the inversion of the linear system produced by quadrature. *J. Assoc. Comput. Mech.* **10**, 97–101.

Yanovskaya, T. B. and Ditmar, P. G. 1990. Smoothness criteria in surface wave tomography. *Geophys. J. Int.* **102**, 63–72.